Theoretical Analysis of the Hydrogen-Transfer Reaction to C═N, C═C, and C≡C Bonds Catalyzed by Shvo's Ruthenium Complex

Aleix Comas-Vives, Gregori Ujaque,* and Agustí Lledós*

Unitat de Química Física, Departament de Química, Universitat Autònoma de Barcelona, 08193 Bellaterra, Catalonia, Spain

Received October 5, 2007

The Shvo catalyst $\{[Ph_4(\eta^5\text{-}C_4CO)]_2H\}Ru_2(CO)_4H$ belongs to the so-called bifunctional catalysts, containing one hydride (bonded to Ru) and one proton (bonded to a ligand), which are easily transferred. The mechanism of hydrogenation of polar double bonds by Shvo's catalyst has been extensively studied; however, imine hydrogenation is still a controversial topic. The outer-sphere mechanism (without substrate coordination) and the inner-sphere mechanism (with substrate coordination) are the two main proposals. Several experimental observations account for each proposed mechanism, besides a theoretical analysis of their respective suggested mechanism. In the present work inner- and outer-sphere mechanisms for hydrogenation of C═N, C═C, and C≡C bonds are analyzed and compared by means of theoretical calculations, complementing our previous work in C═O hydrogenation. The obtained energy profiles support an outer-sphere mechanism in all the cases.

Introduction

The homogeneous hydrogenation of polar double bonds is a widely employed reaction in synthetic chemistry.[1] Industrially, it offers an alternative over classical reducing agents such as $NaBH_4$ and $LiAlH_4$ for its better atom economy, cleaner synthesis, and easier workup procedures, also providing milder conditions and better functional tolerance and chemoselectivity over heterogeneous catalysis. In addition, H_2 is not the only source to perform hydrogenation, and other molecules such as alcohols are also used as hydrogen source.[1,2]

Concerning the hydrogen-transfer mechanism, most transition-metal catalysts operate through the "hydridic route" via a metal-hydride intermediate.[3] The "direct transfer" (without participation of a metal-hydride intermediate) is thought to operate for main group elements. In some transition-metal-catalyzed hydrogenations, the so-called "ionic mechanism" has been proposed for systems involving the addition of H_2 in the form of formally H^+ and H^- species.[4] In this sense, the metal−ligand bifunctional hydrogenation catalysts are those containing two hydrogens with hydridic and acidic character, respectively.[5] The hydridic hydrogen is attached to the metal, whereas the acidic hydrogen is provided by one ligand. One of the most paradigmatic examples of this type of catalysts is the Shvo catalyst[6,7] $\{[Ph_4(\eta^5\text{-}C_4CO)]_2H\}Ru_2(CO)_4H$ (**1**), which has been very versatile and used for a great variety of processes involving hydrogen transfer.[6−15] The bimetallic dimer **1** decomposes upon heating, producing the species **A** and **B**, which are able to perform hydrogenation and dehydrogenation processes, respectively (Scheme 1). A modification of the Shvo tolyl analogue with the exchange of one CO by one PPh_3, $[2,5\text{-Ph-}3,4\text{-Tol}_2(\eta^5\text{-}C_4COH)]Ru(CO)(PPh_3)H$, has recently appeared.[16,17]

Scheme 1. Equilibrium of the Shvo Catalyst

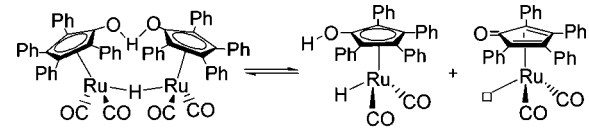

* Corresponding authors. E-mail: gregori@klingon.uab.es; agusti@klingon.uab.es.

(1) *Handbook of Homogeneous Hydrogenation*; de Vries, J. G., Elsevier, C. J., Eds.; Wiley-VCH: Weinheim, 2007.

(2) *Homogeneous Hydrogenation*; Chaloner, P. A., Esteruelas, M. A., Joó, F., Oro, L. A., Eds.; Kluwer Academic Publishers: Dordrecht, 1994.

(3) (a) Gladiali, S.; Alberico, E. *Chem. Soc. Rev.* **2006**, *35*, 226–236. (b) Samec, J. S. M.; Bäckvall, J.-E.; Andersson, P. G.; Brant, P. *Chem. Soc. Rev.* **2006**, *35*, 237–248.

(4) (a) Bullock, R. M. In *Handbook of Homogeneous Hydrogenation*; de Vries, J. G., Elsevier, C. J., Eds.; Wiley-VCH: Weinheim, 2007; Vol. 1, p 153. (b) Bullock, R. M. *Chem.−Eur. J.* **2004**, *10*, 2366–2374. (c) Guan, H.; Iimura, M.; Magee, M. P.; Norton, J. R.; Zhu, G. *J. Am. Chem. Soc.* **2005**, *127*, 7805–7814.

(5) (a) Noyori, R.; Ohkuma, T. *Angew. Chem.* **2001**, *113*, 40–75. *Angew. Chem. Int. Ed.* **2001**, *40*, 40−73. (b) Sandoval, C. A.; Ohkuma, T.; Muñiz, K.; Noyori, R. *J. Am. Chem. Soc.* **2003**, *125*, 13490–13503. (c) Fujii, A.; Hashiguchi, S.; Uematsu, N.; Ikariya, T.; Noyori, R. *J. Am. Chem. Soc.* **1996**, *118*, 2521–2522. (d) Uematsu, N.; Fujii, A.; Hashiguchi, S.; Ikariya, T.; Noyori, R. *J. Am. Chem. Soc.* **1996**, *118*, 4916–4917.

(6) (a) Blum, Y.; Czarkie, D.; Rahamim, Y.; Shvo, Y. *Organometallics* **1985**, *4*, 1459–1461. (b) Shvo, Y.; Czarkie, D.; Rahamim, Y. *J. Am. Chem. Soc.* **1986**, *108*, 7400–7402.

(7) Bullock, R. M. In *Handbook of Homogeneous Hydrogenation*; de Vries, J. G., Elsevier, C. J., Eds.; Wiley-VCH: Weinheim, 2007; Vol. 1, pp 186−193.

(8) Karvembu, R.; Prabhakaran, R.; Natarajan, K. *Coord. Chem. Rev.* **2005**, *249*, 911–918.

(9) Shvo, Y.; Goldberg, I.; Czierkie, D.; Reshef, D.; Stein, Z. *Organometallics* **1997**, *16*, 133–138.

(10) Menashe, N.; Salant, E.; Shvo, Y. *J. Organomet. Chem.* **1996**, *514*, 97–102.

(11) Samec, J. S. M.; Bäckvall, J.-E. *Chem.−Eur. J.* **2002**, *8*, 2955–2961.

(12) Csjernyk, G.; Éll, A. H.; Fadini, L.; Pugin, B.; Bäckvall, J.-E. *J. Org. Chem.* **2002**, *67*, 1657–1662.

(13) (a) Samec, J. S. M.; Éll, A. H.; Bäckvall, J.-E. *Chem.−Eur. J.* **2005**, *11*, 2327–2334. (b) Éll, A. H.; Samec, J. S. M.; Brasse, C.; Bäckvall, J.-E. *Chem. Commun.* **2002**, 1144–1145.

(14) (a) Larsson, A. L. E.; Persson, B. A.; Bäckvall, J.-E. *Angew. Chem.* **1997**, *109*, 1256–1258; *Angew. Chem., Int. Ed.* **1997**, *36*, 1211−1212. (b) Persson, B. A.; Larsson, A. L. E.; Ray, M. L.; Bäckvall, J.-E. *J. Am. Chem. Soc.* **1999**, *121*, 1645–1650.

(15) Paetzold, J.; Bäckvall, J.-E. *J. Am. Chem. Soc.* **2005**, *127*, 17620–17621.

10.1021/om700975k CCC: $40.75
Publication on Web 09/13/2008

Scheme 2. Proposed Catalytic Cycle for Alkyne Hydrogenation (left); Formation of Species D Poisons the Catalyst (right)

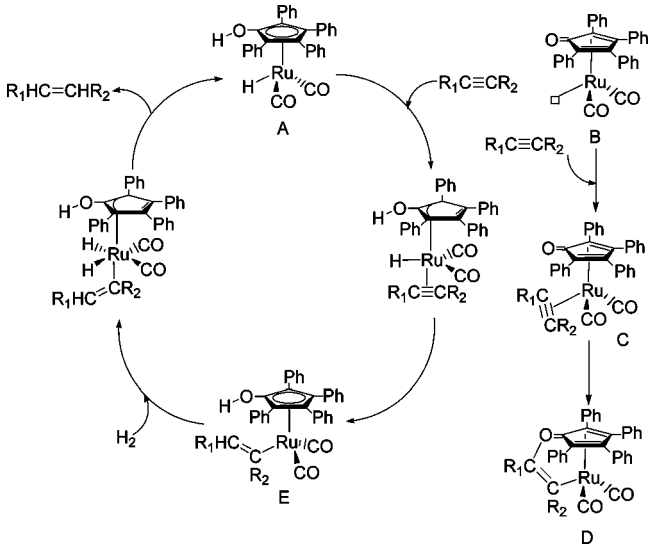

The Shvo catalyst is able to hydrogenate polar (C═O, C═N) and nonpolar double and triple bonds (C═C, C≡C), though it is more efficient for the former. The reaction mechanism for these processes, however, is a matter of controversy. For alkyne hydrogenation Shvo proposed a catalytic cycle involving CpOH ring slippage (see Scheme 2).[9] The formation of a very stable species (labeled as **D** in Scheme 2) poisoned the catalyst. In the same work Shvo suggested that an analogous catalytic cycle may be considered for alkene hydrogenation. Moreover, for alkene hydrogenation, Casey suggested a different mechanism with initial loss of one CO molecule, followed by alkene coordination and hydride transfer, and finally one H_2 molecule performs the cleavage of the Ru-alkyl intermediate, producing alkane.[18]

For the case of C═O hydrogenation mainly two different mechanisms were proposed, where the hydride and proton transfers took place concertedly: (i) outer-sphere mechanism and (ii) inner-sphere mechanism; the latter mechanism involves coordination of the substrate along with the CpOH ring slippage. In this case, however, theoretical calculations clearly support the outer-sphere mechanism.[19a,20]

Concerning imine hydrogenation analogous inner- and outer-sphere mechanisms have been also proposed (Scheme 3). Casey and co-workers suggest a change in the rate-limiting step of imine hydrogenation depending on the substituents on nitrogen.[21] For electron-withdrawing substituents the high reported kinetic isotope effect brings them to conclude that the concerted hydrogen transfer is the rate-limiting step. In contrast, for electron-donating alkyl substituents they observed inverse kinetic isotope effects, deuterium scrambling, and isomerization, concluding that in this case the rate-limiting process was amine coordination on the Ru atom and that hydrogenation was reversible. Since proton and hydride transfer occurred prior to amine coordination, it was not possible to discern using mechanistic information if those processes occurred via a concerted or a stepwise process. Nevertheless, the combination of successful intramolecular trapping besides the failure of the intermolecular one was given as proof against the ring-slippage mechanism (inner-sphere mechanism).[19] They assumed that nitrogen coordination of the newly generated amine was faster than breaking the hydrogen bond between the products, diffusion from the solvent cage, or inversion of the nitrogen lone pair. The same group reported different stereochemistry for the hydrogen transfer depending on the nature of the imine. For N-aryl imines the process was shown to be trans stereoespecific.[22] The N-alkyl imine hydrogenation however was a stereorandom process attributed to a reversible dehydrogenation faster than amine coordination to the metal. Amine escape from the solvent cage and inversion of the nitrogen were considered to be slower than dehydrogenation and amine coordination to the ruthenium.

Scheme 3. Proposed Mechanisms for Polar Double-Bond Hydrogenation

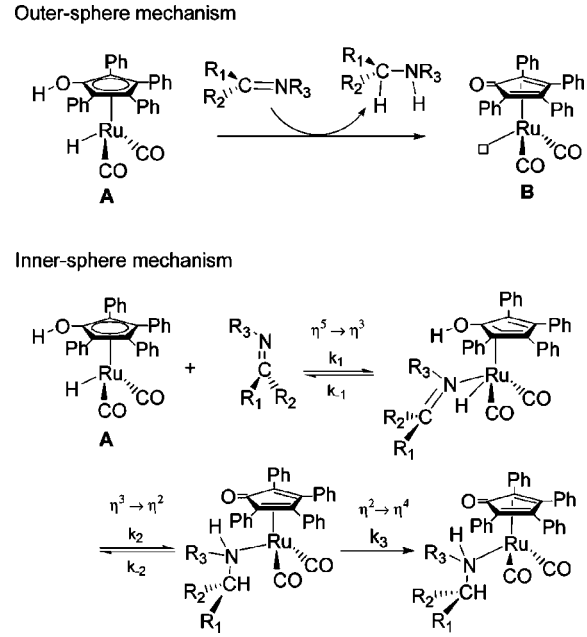

The inner-sphere mechanism proposed by Bäckvall (Scheme 3) starts with the imine-promoted $\eta^5 \rightarrow \eta^3$ CpOH ring slippage allowing imine coordination. The following steps are hydrogenation and the $\eta^2 \rightarrow \eta^4$ rearrangement giving the corresponding amine complex.[23] For the catalytic transfer dehydrogenation of *N*-phenyl-*N*-(1-phenylethylamine) the large reported kinetic isotope effect for the C−H cleavage (3.24) besides the fact that the combined isotope effect (C−H and N−H cleavages) is practically the same (3.26) brought the authors to the conclusion that transfer dehydrogenation of an amine is stepwise, the hydride transfer being the rate-limiting step.[24] In the stochiometric reduction of *N*-phenyl-[1-(4-methoxyphenyl)ethylidene]-amine they suggested that the hydrogen-transfer process was

(16) Casey, C. P.; Strotman, N. A.; Beetner, S. E.; Johnson, J. B.; Priebe, D. C.; Vos, T. E.; Khodavandi, B.; Guzei, I. A. *Organometallics* **2006**, *25*, 1230–1235.

(17) Casey, C. P.; Strotman, N. A.; Beetner, S. E.; Johnson, J. B.; Priebe, D. C.; Guzei, I. A. *Organometallics* **2006**, *25*, 1236–1244.

(18) Casey, C. P.; Singer, S. W.; Powell, D. R. *Can. J. Chem.* **2001**, *79*, 1002–1011.

(19) (a) Casey, C. P.; Bikzhanova, G. A.; Cui, Q.; Guzei, I. A. *J. Am. Chem. Soc.* **2005**, *127*, 14062–14071. See also Supporting Information therein. (b) Casey, C. P.; Clark, T. B.; Guzei, I. A. *J. Am. Chem. Soc.* **2007**, *129*, 11821–11827.

(20) Comas-Vives, A.; Ujaque, G.; Lledós, A. *Organometallics* **2007**, *26*, 4135–4144.

(21) Casey, C. P.; Johnson, J. B. *J. Am. Chem. Soc.* **2005**, *127*, 1883–1894.

(22) Casey, C. P.; Bikzhanova, G. A.; Guzei, I. A. *J. Am. Chem. Soc.* **2006**, *128*, 2286–2293.

(23) Samec, J. S. M.; Ell, A. H.; Åberg, J. B.; Privalov, T.; Eriksson, L.; Bäckvall, J.-E. *J. Am. Chem. Soc.* **2006**, *128*, 14293–14305.

(24) Éll, A. H.; Johnson, J. B.; Bäckvall, J.-E. *Chem. Commun.* **2003**, 1652–1653.

not the rate-limiting step on the basis on the low reported combined isotope effect (1.05).[25] The same group also performed trapping experiments, which support the inner-sphere mechanistic proposal because using an internal amine trap gave only the Ru complex with the newly formed amine from the imine at low temperatures.[23,26]

Different theoretical studies have addressed a mechanistic analysis.[19a,23,27] Casey and co-workers focused on the concerted outer-sphere mechanism for a model imine (H_2C═N-CH_3) and a model catalyst. This mechanism was reported to be feasible with an energy barrier of 4.8 kcal/mol including solvent effects (THF) by means of single-point IEF-PCM calculations.[19a] Privalov, Samec, and Bäckvall analyzed the inner-sphere mechanism. Calculations were performed taking an electron-donating imine ((CH_3)$_2$C═N-CH_3) and the complete catalyst including solvent effects by PCM and explicit solvent molecules. The reported energy barrier was 15 kcal/mol, corresponding to imine coordination coupled with ring slippage. The following steps, hydride transfer and $\eta^2 \rightarrow \eta^4$ ring slippage, were found to be similar but lower in energy. They suggested that any of these steps may become rate-limiting depending on the electronic nature of the imine.[27]

Given all these different and contraposed mechanistic considerations and following our previous mechanistic studies on the hydrogenation using Shvo's catalyst[20] we decided to perform an extensive analysis of the reaction mechanism for imines, alkenes, and alkynes by means of theoretical calculations. Our aim is to perform an unbiased comparative theoretical study of both inner- and outer-sphere mechanisms for these substrates in order to cast light on new evidence trying to discern between these pathways.

Computational Details

Calculations were carried out using the program package Gaussian03[28] at density functional theory (DFT) level by means of the hybrid B3LYP functional.[29]

Mechanistic analysis was performed extensively by using a model reaction system. We used as substrates the simplest species containing C═N, C═C, and C≡C groups, methanimine, ethylene, and acetylene, respectively. The Shvo catalyst was modeled by [(η^5-C_4H_4COH)Ru(CO)$_2$H]; the phenyl substituents of the aromatic ligand, hereafter named CpOH, were replaced by hydrogens. These four H's were calculated using the 6-31G basis set and the other main group elements (C, N, the rest of H) were calculated using the 6-31G(d,p) basis set. For the case of imine hydrogenation, a model taking the complete catalyst [(η^5-C_4Ph_4COH)Ru(CO)$_2$H] along with an example of electron-donating imine [H_3C-N═C(CH_3)$_2$] was also evaluated; the 6-31G(d,p) basis set was used for all the atoms except the Ru, which was described by the LANL2DZ effective core potential[30] and its associated basis set for the outermost electrons. To check the basis set dependence, single-point calculations using a larger basis set were performed:

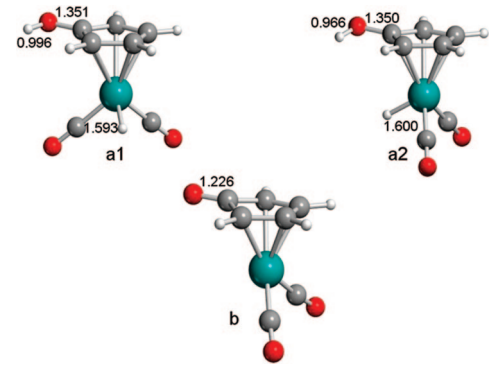

Figure 1. Optimized structures for the initial and final catalyst. The two rotamers for the initial catalyst, **a1** and **a2**, are depicted. Distances are in Å.

the 6-311++G(d,p) basis set was used for C, N, O, and H and f polarization functions were added to the Ru atom using the lanl2dz pseudopotential. No significant changes were observed when increasing the basis set (see Supporting Information).

For the saddle points the existence of only one imaginary frequency was checked by means of frequency calculations. The IRC approach was used to corroborate the minima linked by every transition state.[31] Solvent effects (THF, $\varepsilon = 7.58$) were included using CPCM[32] single-point calculations. For the hydrogens directly involved in the reaction the SPHEREONH option was used in order to place individual cavities on them. Some steps for imine hydrogenation mechanisms (indicated in the text) were evaluated reoptimizing the structures including the solvent effects by means of the CPCM method.

Results and Discussion

This section is divided into two subsections, which analyze imine and both alkene and alkyne hydrogenation mechanisms, respectively. In all of them both inner- and outer-sphere mechanisms are evaluated. The inner-sphere mechanisms require the coordination of the substrate to the catalyst, whereas in the outer-sphere mechanism the hydrogenation occurs by simultaneous hydride and proton transfer to the substrate without coordination to the metal.

In our previous study[20] two rotamers were also localized for the active reducing species of the Shvo catalyst, **a1** and **a2**. These structures besides the final dehydrogenated catalyst **b** are depicted in Figure 1. These two conformers differ energetically only by 0.2 kcal/mol, indicating that the different rotamers are equally accessible. Only the **a2** rotamer is considered in this study.

Once the hydrogenation takes place, the dehydrogenated form of the catalyst (**b**) and the hydrogenated product, methylamine, ethane, and ethene are produced. The reaction energies for the imine, alkene, and alkyne hydrogenation are −6.4, −15.4, and −27.3 kcal/mol in the gas phase, respectively. In solution these energies do not change significantly: −9.0, −17.7, and −28.9 kcal/mol. For formaldehyde hydrogenation we reported values of −0.2 and −3.7 kcal/mol in the gas phase and solution, respectively.[20]

Imine Hydrogenation. Inner-Sphere Mechanisms. These mechanisms require the creation of a vacant site in order to

(25) Samec, J. S. M.; Él l, A. H.; Bäckvall, J.-E. *Chem. Commun.* **2004**, 2748–2749.

(26) Bäckvall considers that hydrogen transfer to electron-deficient imines should be faster than to electron-rich ones, whereas the newly formed amine coordination should be slower in case the outer-sphere mechanism was the operative one.

(27) Privalov, T.; Samec, J. S. M.; Bäckvall, J.-E. *Organometallics* **2007**, *26*, 2840–2848.

(28) Frisch, M. J.; et al. *Gaussian03*; Gaussian, Inc.: Wallingford, CT, 2004.

(29) (a) Becke, A. D. *J. Chem. Phys.* **1993**, *98*, 5648–5652. (b) Lee, C.; Yang, W.; Parr, R. G. *Phys. Rev. B* **1988**, *37*, 785–789. (c) Stephens, P. J.; Devlin, F. J.; Chabalowski, C. F.; Frisch, M. J. *J. Phys. Chem.* **1994**, *98*, 11623–11627.

(30) Hay, P. J.; Wadt, W. R. *J. Chem. Phys.* **1985**, *82*, 270–283.

(31) (a) Fukui, K. *Acc. Chem. Res.* **1981**, *14*, 363–368. (b) Gonzalez, C.; Schlegel, H. B. *J. Chem. Phys.* **1989**, *90*, 2154–2161. (c) Gonzalez, C.; Schlegel, H. B. *J. Phys. Chem.* **1990**, *94*, 5523–5527.

(32) (a) Barone, V.; Cossi, M. *J. Phys. Chem. A* **1998**, *102*, 1995–2001. (b) Cossi, M.; Rega, N.; Scalmani, G.; Barone, V. *J. Comput. Chem.* **2003**, *24*, 669–681.

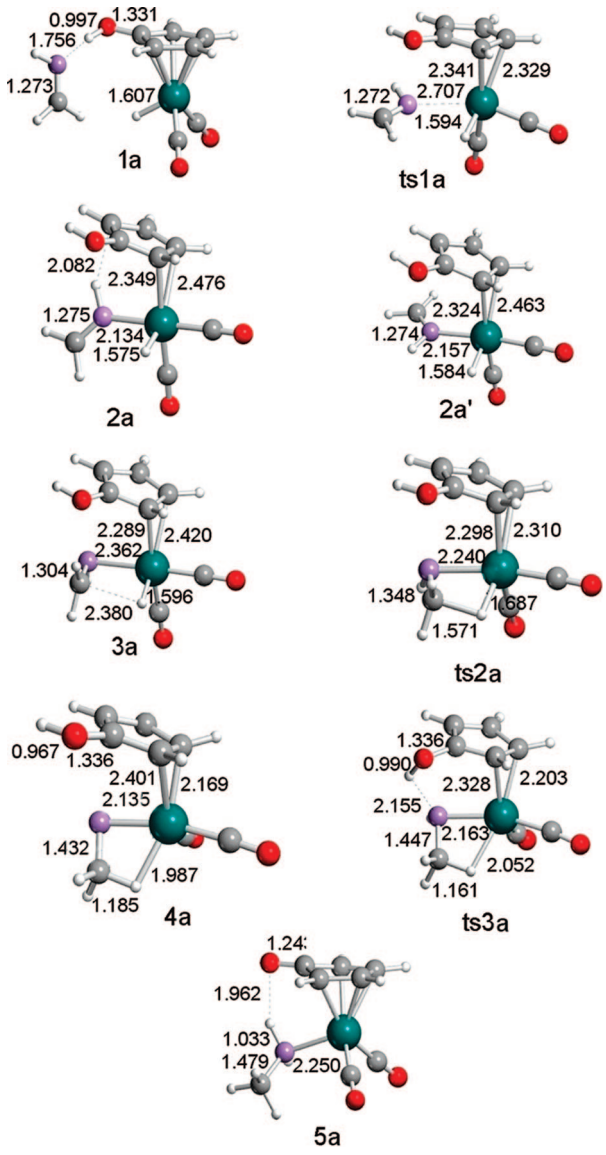

Figure 2. Located stationary points for the stepwise $\eta^5 \rightarrow \eta^2$ ring-slippage mechanism of $H_2C{=}NH$ hydrogenation. Distances are in Å.

coordinate the substrate species. For the creation of a vacant site by a CO leaving we reported an initial energy cost of 45.7 kcal/mol in CPCM with THF as solvent and 38.7 kcal/mol for the free energy difference in the gas phase.[20] Thus, we did not further consider this mechanism. In this line, Casey and co-workers found noticeable CO exchange only under fluorescent light.[33]

***$\eta^5 \rightarrow \eta^2$* Stepwise Mechanism.** In this stepwise mechanism we considered as a first step the $\eta^5 \rightarrow \eta^2$ ring slippage of the CpOH ring, allowing the imine coordination. In Figure 2 are shown all the located stationary points of this pathway for the model catalyst and the simplest imine.

In the intermediate **2a** the imine group is η^1 coordinated to the metal through the N atom of the imine ligand with a Ru−N distance of 2.134 Å. Two carbons of the CpOH group remains attached to the Ru atom, having Ru−C distances of 2.349 and 2.476 Å. A recent theoretical study showed that the η^2 coordination mode of the Cp was the most stable upon ligand addition on related transition-metal complexes.[34] This coordination mode was also found in some ligand addition transition states.[35]

The first transition state involves the $\eta^5 \rightarrow \eta^2$ CpOH ring slippage (**ts1a**) along with the η^1-imine coordination producing intermediate **2a**. The relative barrier height is considerably high, 27.4 kcal/mol with respect to the hydrogen-bonded adduct of the reactants (**1a**). This transition state is characterized by a Ru−N distance of 2.707 Å and Ru−C distances for the incoming coordinated carbons of the CpOH ring of 2.341 and 2.329 Å. In the Figure 3 are shown the energy profiles for this pathway both in the the gas phase and solution.

From **2a** to **2a′** there is a rotation of the imine ligand that facilitates the subsequent steps.[36] Once the intermediate **2a′** is formed, there are two ways to proceed from this intermediate: first proton transfer followed by hydride transfer or first hydride transfer followed by proton transfer. We calculated the direct proton transfer, reporting a transition state located at 33.1 kcal/mol with respect to our origin of energies (this is 46.7 kcal/mol with respect to the **1a** structure). This result leads us to discard this option, in favor of the hydride transfer followed by the proton transfer (vide infra).

For the hydride migration to the carbon of the imine, the coordination mode of the imine changes to a η^2 coordination mode (**3a**), with Ru−C and Ru−N distances of 2.510 and 2.362 Å, respectively. This change is thermodynamically noticeable in the imine case, 13.8 kcal/mol, confirming the known preference of imines for a η^1 mode of coordination over the η^2 one. The relative barrier height for the hydride migration (**ts2a**) is only 3.9 kcal/mol, producing species **4a**, located at 21.8 kcal/mol on the potential energy surface. The intermediate **4a** is characterized by an agostic interaction with C−H and Ru−H distances of 1.185 and 1.987 Å, respectively. Finally, the proton transfer from the CpOH group to the iminic N atom has a relative barrier of 3.2 kcal/mol, giving the final product **5a**. This step is highly exothermic (60.6 kcal/mol) with a relative energy in the complete energy profile (Figure 3) of −38.8 kcal/mol.

As shown in Figure 3 the highest energy points in the complete gas-phase pathway are hydride and proton-transfer processes, having similar energies of 25.2 and 25.0 kcal/mol, respectively. Thus, the overall energy barrier is 38.8 kcal/mol (40.4 kcal/mol in solution). The energy profile is not significantly affected by considering solvent effects (THF); the differences are not higher than 5 kcal/mol. Both hydride and proton transfer show similar energy barriers in the gas phase and solution.

For the model system studied the relative energy values obtained by single-point CPCM calculations for **1a**, **2a′**, **4a**, and **5a** are −10.8, 8.7, 24.9, and −37.9 kcal/mol, respectively. In order to check the molecular model employed, the previous points were reoptimized in solution including the phenyl rings of the catalyst (complete catalyst), obtaining values of −8.6, 9.5, 25.5, and −37.2 kcal/mol, respectively. Thus, the full geometry reoptimization performed in solvent and taking the complete catalyst does not significantly change the results for this $\eta^5 \rightarrow \eta^2$ mechanism.

(33) Casey, C. P.; Singer, S. W.; Powell, D. R.; Hayashi, R. K.; Kavana, M. *J. Am. Chem. Soc.* **2001**, *123*, 1090–1100.

(34) Veiros, L. F. *Organometallics* **2000**, *19*, 5549–5558.

(35) Fan, H.-J.; Hall, M. B. *Organometallics* **2001**, *20*, 5724–5730.

(36) The reaction profile starting from structure **2a** was also analyzed. A new transition state, **ts2an**, analogous to **ts2a** was characterized. Nevertheless, this transition state is higher in energy compared to **ts2a** (27.5 vs 25.2 kcal/mol). A structure analogous to **3a** (labeled as **3an**) was also found for this pathway with a relative energy of 18.2 kcal/mol.

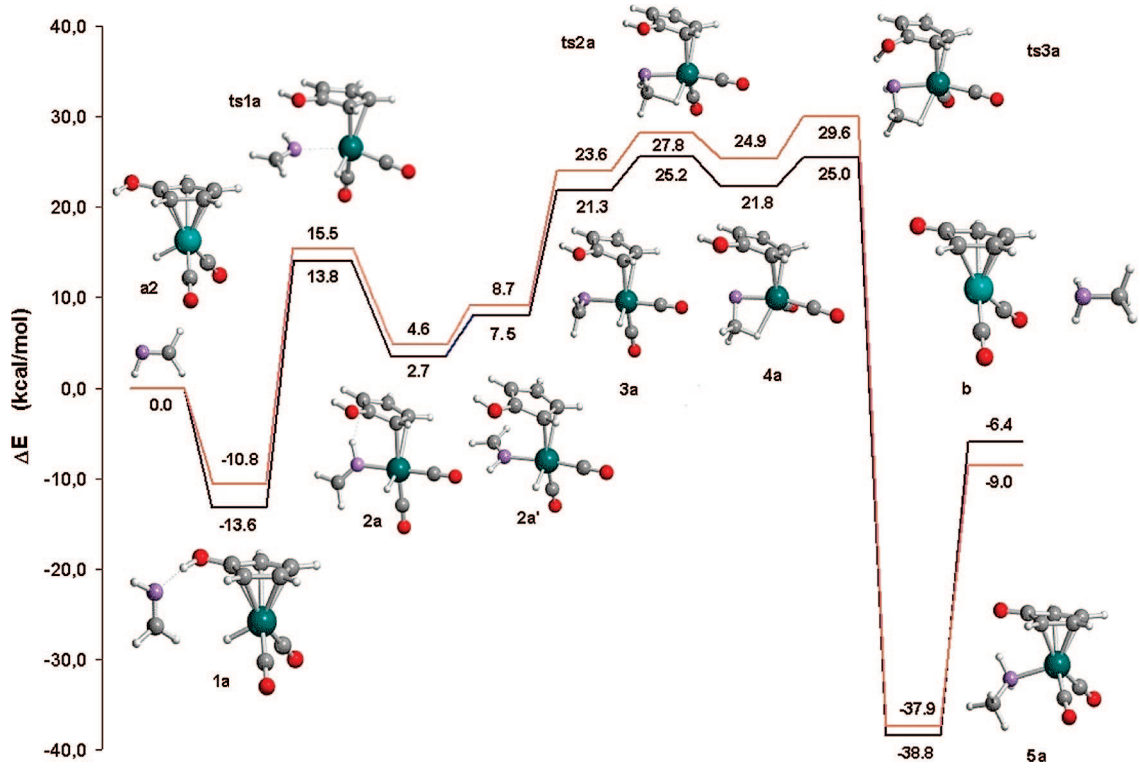

Figure 3. Energy profile for the stepwise $\eta^5 \rightarrow \eta^2$ ring-slippage mechanism of $H_2C{=}NH$ hydrogenation in the gas phase (blue) and solution (orange).

***$\eta^5 \rightarrow \eta^3$* Concerted Mechanism.** In the case of carbonyl hydrogenation and using an analogous model system, we reported a transition state structure for a concerted hydride and proton transfer with an η^3-CpOH coordination to the metal.[20] In the present case, however, we were unable to localize an analogous transition state for imine hydrogenation. This fact may suggest that for the model system, if existing, this mechanism would be too energy demanding to be a reasonable pathway, as we actually found in carbonyl hydrogenation, with a relative barrier height in the gas phase of 36.0 kcal/mol.[20]

This particular reaction mechanism, a concerted $\eta^5 \rightarrow \eta^3$ mechanism, has been already theoretically analyzed in detail by Privalov, Samec, and Bäckvall utilizing an imine with electron-donating groups and a complete catalyst model.[27] In their analysis, where solvent effects were included by a combination of explicit solvent molecules (CH_2Cl_2) and a polarized continuum method, they found that the highest energy barrier for this mechanism corresponds to the first step: the σ-bond imine coordination concomitantly to the $\eta^5 \rightarrow \eta^3$ CpOH ring slippage. Subsequently, they proposed a fast proton transfer followed by a slower hydride transfer. Finally, the $\eta^2 \rightarrow \eta^4$ ring slippage takes place. All the steps presented lower but quite similar activation barriers than the initial imine coordination. The authors showed that the inclusion of solvent effects stabilizes the low-hapticity complexes, and in fact, the lowest energy reaction barrier (15 kcal/mol) was obtained when explicit solvent molecules (along with the continuum model) were included in the calculations. According to their results, this could be a reasonable pathway for the reaction.

Outer-Sphere Mechanism. In the outer-sphere mechanism the hydrogenation takes place concertedly outside the coordination sphere of the metal. Figures 4 and 5 present the localized stationary points and the reaction energy profile, respectively.

The initial structure **1a** is 13.6 kcal/mol lower in energy compared to separated reactants, mainly due to a hydrogen-bond interaction. The concerted hydride and proton transfer (**ts1b**) has a relative barrier height of 11.0 kcal/mol (9.6 kcal/mol in solution). In the product (**2b**) the recently formed C−H bond is interacting with the Ru atom, whereas the aminic N−H bond is interacting with the recently formed C=O bond of the CpO ring.

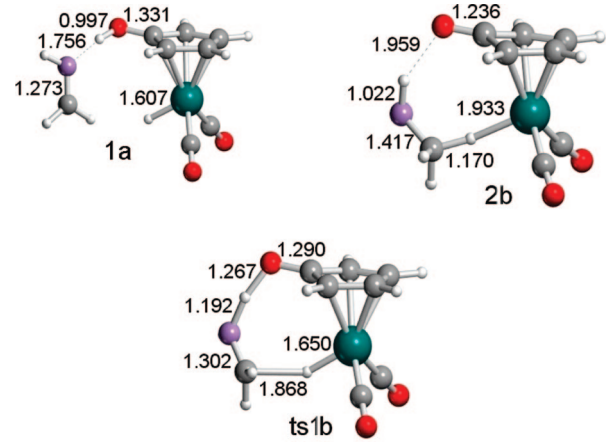

Figure 4. Optimized structures for the concerted outer-sphere mechanism of $H_2C{=}NH$ hydrogenation. Distances are in Å.

For the model imine the concerted hydrogen-transfer pathway is by far more favorable (11.0 kcal/mol) than the $\eta^5 \rightarrow \eta^2$ stepwise mechanism (38.8 kcal/mol).

Given the fact that the presence of the Ph groups on the aromatic ligands of the catalyst has been suggested to help the ring-slippage mechanism[27] and that this mechanism was already studied using a complete catalyst, we decided to investigate the concerted pathway employing also the complete catalyst.

When including phenyl rings in the catalyst, a concerted transition state was also found with a barrier height of 9.3 kcal/

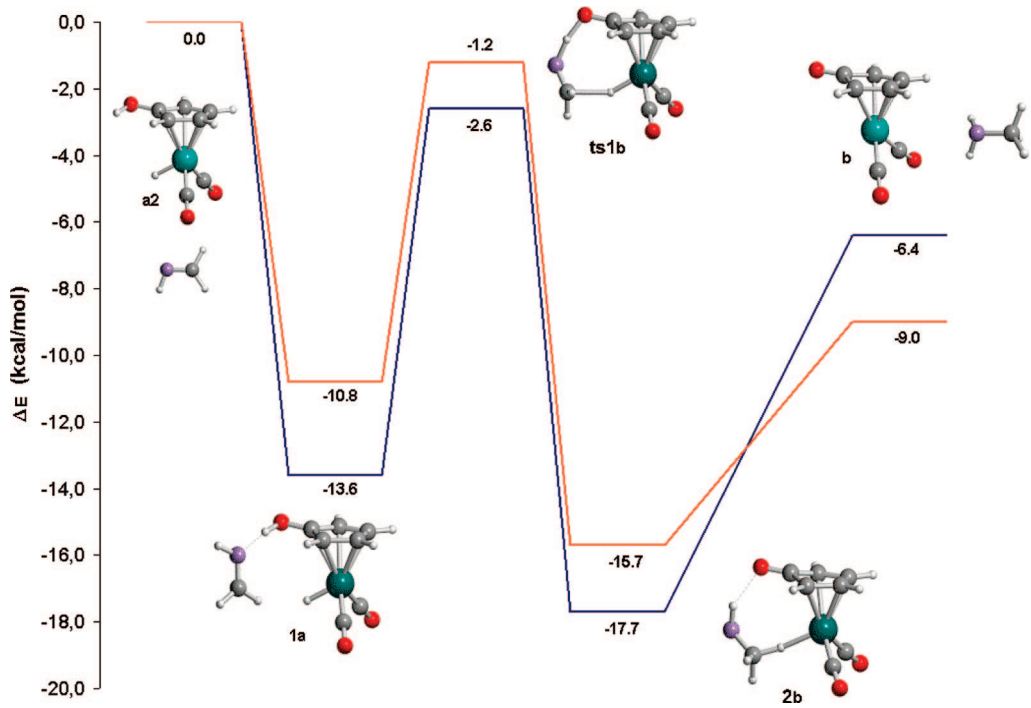

Figure 5. Energy profile for the concerted outer-sphere mechanism of $H_2C{=}NH$ hydrogenation in the gas phase (blue) and solution (orange).

mol in the gas phase. In this transition state, the proton is slightly more transferred to the substrate compared to the model system, having O−H (CpOH group) and N−H distances of 1.299 and 1.178 Å, respectively, whereas the hydride is slightly less transferred, with respective C−H and Ru−H distances of 1.898 and 1.646 Å, respectively. These results are analogous to those found in carbonyl hydrogenation, where the inclusion of the phenyl rings did not change significantly the energy profile of the concerted outer-sphere mechanism.[20] When single-point CPCM calculations are performed the energy barrier diminishes, taking a final value of 7.1 kcal/mol. In addition, in order to check whether performing the geometry optimization in solution changes the results, we reoptimized the complete catalyst within the CPCM methodology in THF. The energy barrier obtained (6.8 kcal/mol) does not change significantly with respect to the single-point solvent calculations. When comparing the transition-state geometry optimized in solution with respect to the gas phase one (values presented in parentheses), the geometrical trend is even more pronounced than that observed when including the phenyl rings in the model system. The proton is again in a more advanced stage (more transferred to the iminic nitrogen), whereas the hydride transfer is in an earlier stage (less transferred to the iminic carbon). The N−H bond and the O−H bond distances of the CpOH group are 1.084 (1.178) and 1.505 Å (1.299 Å), whereas the C−H and Ru−H bonds distances are 2.077 (1.898) and 1.642 Å (1.646 Å); values in parentheses are those of the model system in the gas phase. Thus, although the energy profile does not significantly change the geometry of the transition state, it does change when including the phenyl rings and optimizing in solution, resulting in a concerted but significantly asynchronic transition state. This geometrical trend observed when improving both the model and the methodology opens the door to a stepwise mechanism with an initial proton transfer followed by a hydride transfer for some particular systems.

In any case, according to all these results, the hydrogen transfer to imines will be through an outer-sphere mechanism. In order to check whether this conclusion is also valid for electron-donating imines, we calculated the energy profile for $(CH_3)_2C{=}N\text{-}CH_3$, taking the complete catalyst (including phenyl rings) and optimizing the structures in solvent (THF). On the basis of our results the outer-sphere mechanism is also the most favorable mechanism for this electron-rich imine, with energy barriers of 6.1 and 4.0 kcal/mol, in the gas phase and solution (optimizing geometries in both cases), respectively.

This result is consistent with that obtained by Casey and co-workers on a model system using $H_2C{=}N\text{-}CH_3$ as imine. They obtained a barrier height of 4.8 kcal/mol by performing single-point MP2 calculations over B3LYP-optimized geometries including solvent effects by means of the PCM method.[19a] The energy barrier for the outer-sphere mechanism is more than 10 kcal/mol lower in energy than the lowest barrier reported for the inner-sphere mechanism,[27] using a similar computational methodology (15.0 kcal/mol).

The presence of electron-donating groups increases the basicity of the imine. This could explain the advanced stage of the proton transfer to the nitrogen in the transition-state structure (**ts1c**). Concerning the hydride transfer, it is more transferred to the iminic carbon (see Figure 6). Thus, a mechanism involving stepwise proton transfer followed by hydride transfer would be also conceivable for the hydrogenation of electron-donating imines. The general conclusion from all these results is that for the hydrogen transfer to imines a concerted but asynchronic outer-sphere pathway is clearly favored over the inner-sphere mechanisms.

Alkyne and Alkene Hydrogenation. The Shvo catalyst is also active for hydrogenation of alkenes and alkynes. For alkene and ketone hydrogenation (at mainly 145 °C and 500 psi of H_2) Shvo reported turnover numbers of almost 2000 in most cases.[6a] Conversely, for alkyne hydrogenation the turnover numbers were only a few hundreds. The difference of reactivity between nonpolar and polar double bonds was also evaluated by Casey. The cyclohexene reduction by the tolyl analogue **A** (see Scheme 2) took place by heating to 80 °C under 1 atm of

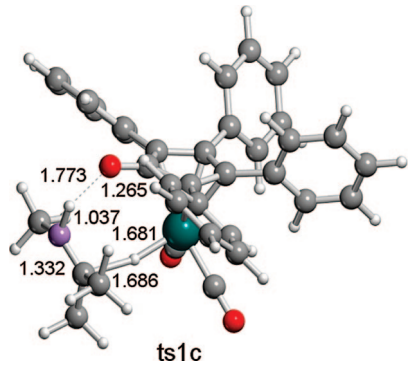

Figure 6. Transition state for the concerted outer-sphere mechanism of $(CH_3)_2C{=}N\text{-}CH_3$ optimized in solution (THF). Distances are in Å.

H_2, reaching only 5 turnovers in 24 h. Nevertheless, the hydrogenation of polar double bonds occurred below room temperature.[33]

Shvo found that alkene hydrogenation was not occurring by using HCO_2H as reducing agent.[10] In another study, Casey and co-workers found that a hydroxycyclopentadienyl ruthenium formate intermediate was not able to perform hydrogenation of benzaldehyde. Only after decarboxylation of the ruthenium formate intermediate was the tolyl analogue **A** formed, which is the active species of hydrogenation. On the basis of their observations, Casey and co-workers suggested that alkene hydrogenation may proceed involving initial loss of CO from the tolyl analogue **A**. Alkene insertion into the Ru−H bond and final cleavage of the H_2 molecule by the Ru-alkyl intermediate to produce the alkane were suggested as subsequent steps.[18]

Concerning alkyne hydrogenations, Shvo isolated by reaction of **1** with the alkyne $C_2(4\text{-Cl-Ph})_2$ an analogous species to the one depicted as **D** in Scheme 3.[9] Isostructural species with several alkynes were obtained and characterized using IR, NMR, and elementary analysis, obtaining also the X-ray crystallographic data for $C_2(4\text{-Cl-Ph})_2$. This species was found to be stable during hydrogenation conditions, its formation being irreversible.

The route that leads to this undesired product (**B** to **D** of Scheme 2) is computationally analyzed using the model catalyst and acetylene as alkyne. The energies in this case are referred to the dehydrogenated form of the catalyst (**b**) and acetylene. The coordination of the alkyne is exothermic by 17.2 kcal/mol and leads to intermediate **c**. The transition step that leads to **d** has a barrier height of 22.8 kcal/mol (23.4 kcal/mol in solution), and the formation of the species **d** is thermodynamically favored by 39.9 kcal/mol (34.8 kcal/mol in solution). We can compare the optimized **d** species with the X-ray diffraction geometry obtained by Shvo and co-workers. The alkyne is σ-bonded through both carbon atoms to the Ru and to the O of the CpO ring, respectively. The experimental Ru−C and C−O distances are 2.114(11) and 1.409(11) Å, respectively,[9] whereas the calculated ones are 2.083 and 1.396 Å, respectively. The X-ray C−C distance is 1.351(17) Å, whereas the calculated one is 1.338 Å, showing an excellent agreement.

The reaction of **1** with the dimethyl acetylenedicarboxylate ($C_2(CO_2Me)_2$) alkyne gave the analogous complex to that depicted as **E** in Scheme 2.[9] This complex was identified within the catalytic cycle. This species is very stable thermodynamically; at 140 °C for 10 h in toluene it does not eliminate the alkene. Nevertheless, with 15 atm of hydrogen pressure at 110 °C in THF it gives back the initial complex **1** and dimethyl succinate (alkane). From these observations, Shvo and co-workers proposed the catalytic cycle shown in Scheme 2. Thus, the oxidative addition of the incoming H_2 molecule followed by a reductive elimination giving the final product and regenerating the catalyst was postulated for closing the catalytic cycle. For the case of alkenes, a similar mechanism was supposed to be operative. Thus, the mechanism for alkyne and alkene hydrogenation was computationally evaluated.

Scheme 4. Reaction Steps of the $\eta^5 \rightarrow \eta^2$ Stepwise Mechanism for Alkynes[a]

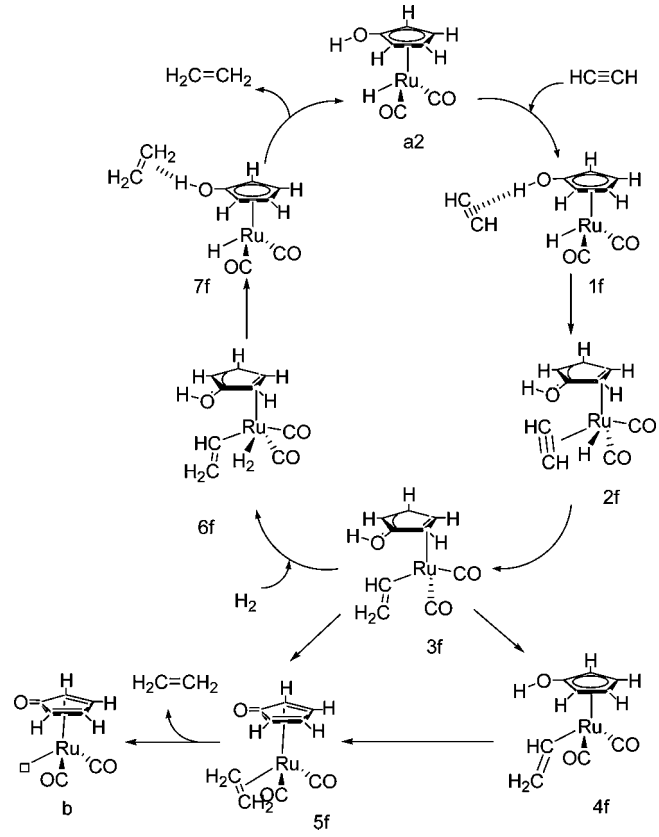

[a] A completely analogous mechanism is found for alkenes. In this case, the initial intermediate is **7f**.

Due to the small reported differences when including the phenyl groups and optimizing in solvent in imine hydrogenation, we studied alkene and alkyne hydrogenation with the simplified catalyst (without phenyl groups) and introducing solvent effects by means of single-point CPCM calculations.

***$\eta^5 \rightarrow \eta^2$* Stepwise Mechanism for Alkyne and Alkene and Hydrogenation.** The evaluation of this mechanism for both alkynes and alkenes shows that the minima and transition states are analogous to those found in the imine hydrogenation parent mechanism up to the first hydride migration. In the first step ($\eta^5 \rightarrow \eta^2$ ring slippage), however, both substrates become directly η^2-coordinated to the metal. The schematic representation of this mechanism for alkynes is depicted in Scheme 4. A completely analogous mechanism is found for alkenes.

The geometries of the transition states for $\eta^5 \rightarrow \eta^2$ CpOH ring slippage with substrate coordination and the subsequent hydride transfer are shown in Figure 7 for both alkyne (**ts1f**, **ts2f**) and alkene (**ts1g**, **ts2g**) hydrogenations. The relative energies for these mechanisms are shown in Table 1 for alkynes and in Table 2 for alkenes.

The $\eta^5 \rightarrow \eta^2$ ring slippage coupled with the corresponding substrate coordination is characterized by Ru−C distances of 2.839 and 2.757 Å in the case of acetylene. Concerning the

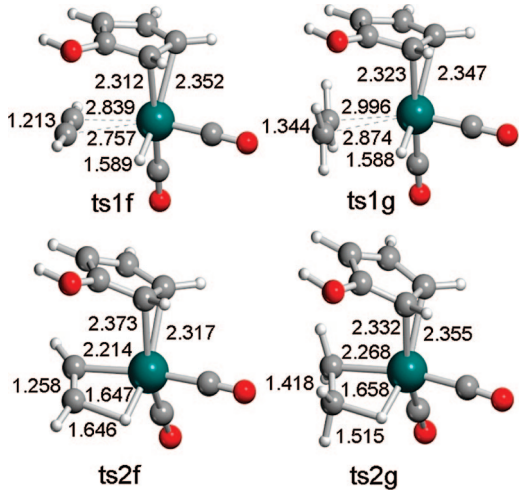

Figure 7. Transition states for the $\eta^5 \rightarrow \eta^2$ CpOH ring slippage and the hydride-transfer steps in alkyne (**ts1f** and **ts2f**, respectively) and alkene (**ts1g** and **ts2g**, respectively) hydrogenations. Distances are in Å.

Table 1. Computed Energies (in kcal/mol) of the $\eta^5 \rightarrow \eta^2$ CpOH Ring-Slippage Mechanism for Alkynes in the Gas Phase (E_{B3LYP}) and Solution (E_{THF})

	structure	E_{B3LYP}	E_{THF}
reactants	**a2** + **HC≡CH**	0.0	0.0
	1f	−6.0	−2.9
$\eta^5 \rightarrow \eta^2$ CpOH ring slippage	**ts1f**	21.8	23.4
	2f	19.7	21.2
hydride transfer	**ts2f**	27.6	29.4
η^2-CpOH alkenyl	**3f**	4.2	6.7
η^5-CpOH alkenyl	**4f**	−37.7	−35.2
proton transfer from the η^5-CpOH	**ts3f**	−3.4	−2.2
product of the proton transfer	**5f**	−49.8	−50.2
products 1	**b** + **H_2C=CH_2**	−27.3	−28.9
hydrogen complex	**6f**	−1.4	−0.5
H_2 σ-bond metathesis	**ts4f**	5.6	6.9
product of the H_2 σ-bond metathesis	**7f**	−58.6	−55.4
products 2	**a2** + **H_2C=CH_2**	−53.7	−53.8

Table 2. Computed Energies (in kcal/mol) of the $\eta^5 \rightarrow \eta^2$ CpOH Ring-Slippage Mechanism for Alkenes in the Gas Phase (E_{B3LYP}) and Solution (E_{THF})

	structure	E_{B3LYP}	E_{THF}
reactants	**a2** + **H_2C=CH_2**	0.0	0.0
	7f	−4.9	−1.6
$\eta^5 \rightarrow \eta^2$ CpOH ring slippage	**ts1g**	22.0	22.7
	2g	18.4	19.0
hydride transfer	**ts2g**	27.2	28.0
η^2-CpOH alkyl	**3g**	19.9	21.3
η^5-CpOH alkyl	**4g**	−18.0	−18.1
proton transfer from the η^5-CpOH	**ts3g**	25.0	25.0
proton transfer from the η^2-CpOH	**ts3g2**	52.9	54.9
product of the proton transfer	**5g**	−19.7	−18.5
products 1	**b** + **H_3C-CH_3**	−15.4	−17.7
hydrogen complex	**6g**	18.1	17.5
H_2 σ-bond metathesis	**ts4g**	24.7	24.5
product of the H_2 σ-bond metathesis	**7g**	−43.2	−41.3
products 2	**a2** + **H_3C-CH_3**	−41.8	−42.6

analogous step for ethene coordination the Ru−C distances present values of 2.996 and 2.874 Å. The transition states for the next step, the insertion into the Ru−H bond, are characterized by C−H distances of 1.646 and 1.515 Å in the case of alkynes (**ts2f**) and alkenes (**ts2g**), respectively.

The relative barrier height in the gas phase for the $\eta^5 \rightarrow \eta^2$ ring slippage coupled with the corresponding substrate coordination is 27.8 (**ts1f**) and 26.9 (**ts1g**) kcal/mol for acetylene and ethene, respectively. Concerning the hydride migration, there are no remarkable changes in the energetics between acetylene and ethene hydrogenations, presenting relatives barrier heights of 7.9 (**ts2f**) and 8.8 (**ts2g**) kcal/mol, respectively. The first remarkable difference comes from the energetics of **3f** and **3g** intermediates (4.2 and 19.9 kcal/mol, respectively), which are the intermediates after the hydride migration for alkynes and alkenes, respectively. In these intermediates, however, the coordinated species are quite different, an alquilidene in **3f** and an ethyl group in **3g**, respectively.

From this point, two different alternatives were found. According to the Shvo mechanism, next step corresponds to the addition of H_2. On the basis of the fact that the experimental analogue of **4f** (that corresponds to **E** in Scheme 2) produces **1** and the corresponding alkane under 15 atm of H_2 at 110 °C in THF, Shvo proposed one intermediate of Ru(IV) after the oxidative addition of one H_2 molecule. The transfer of one hydride was required to fully hydrogenate the substrate. The dihydride species with a formal Ru(IV) species could not be located in the potential surface energy; all the optimizations lead to a dihydrogen complex. Nevertheless, a different pathway involving a σ-bond metathesis of the H_2 molecule was found. We calculated this transition state, and it leads to the final product and regenerates the initial catalyst **a2**. This step is affordable with a relative barrier of 7.0 kcal/mol (**ts4f**) and 6.6 kcal/mol (**ts4g**) from the **6f** and **6g** intermediates for alkynes and alkenes, respectively. The σ-bond metathesis step gives rise to the final product and the regeneration of the initial catalyst (**a2**), a process greatly exothermic: 57.2 and 61.3 kcal/mol for alkynes and alkenes, respectively.

The other alternative consists in the proton transfer from the CpOH group to form the final product. This step can occur with or without previous change in the hapticity of the CpOH ring, changing from an η^2 to an η^5 coordination to the Ru atom. In the case of alkynes the change of hapticity is exothermic by 41.9 kcal/mol and the intermediate obtained (**4f**) is located at −37.7 kcal/mol in the energy profile. The analogous minimum in alkene hydrogenation (**4g**) is located at −18.0 kcal/mol in the energy profile, the change of hapticity being exothermic by 37.9 kcal/mol. The proton-transfer transition state from the η^5-coordinated CpOH ring intermediate (**ts3f**) is located at −3.4 kcal/mol in the energy profile, and it presents a relative barrier height of 34.3 kcal/mol. In the case of alkenes the related transition state is located at 25.0 kcal/mol (**ts3g**) with a relative barrier height of 43.0 kcal/mol. For alkynes this step is exothermic by 12.1 kcal/mol (**5f**), whereas for alkenes the process is almost isoenergetic (**5g**), being exothermic by only 1.7 kcal/mol. In contrast to polar double-bond hydrogenation, in carbon−carbon multiple bonds proton-transfer processes become highly energy demanding steps. This is reasonable taking into account the higher basicity of carbonyl and imine groups than that of the nonpolar double and triple bonds.

In acetylene hydrogenation only the proton transfer of the CpOH group from the **4f** intermediate was localized, where the CpOH ring is η^5 coordinated to the Ru. Conversely, in ethene hydrogenation the proton-transfer processes from both the η^2 and η^5 hapticities of the CpOH ring were analyzed.

Concerning alkene hydrogenation, the absolute energies of the transition states involving the η^5-CpOH proton transfer and the σ-bond metathesis of the H_2 molecule are quite similar (25.0 vs 24.7 kcal/mol). However, the relative barrier heights show that the σ-bond metathesis of the H_2 molecule is favored over the η^5-CpOH proton transfer (6.6 vs 43.0 kcal/mol). In Figure 8 are shown the transition-state geometries for the second hydrogenation step of alkenes and alkynes. These are the proton-

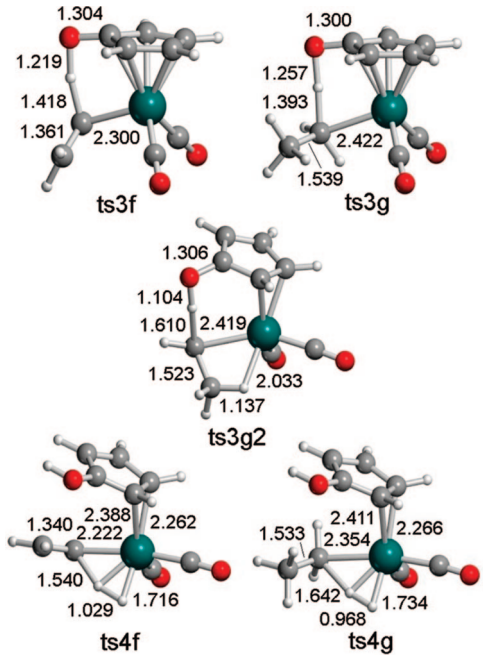

Figure 8. Transition states for the proton transfers from the CpOH ring for alkynes (**ts3f**, only η^5-CpOH ring) and alkenes (**ts3g**, **ts3g2**) and for the σ-bond metathesis of one incoming H_2 molecule for alkynes and alkenes, **ts4f** and **ts4g**, respectively. Distances are in Å.

transfer processes from the CpOH ring for alkynes (**ts3f**) and alkenes (**ts3g** and **ts3g2**) and the σ-bond metathesis of one incoming H_2 molecule (**ts4f** and **ts4g**).

This mechanism is related to that proposed by Shvo; the σ-bond metathesis makes sense within the $\eta^5 \rightarrow \eta^2$ stepwise mechanism because of the lower relative barrier height. Nevertheless, from the **4f** analogue the barrier is higher than for the η^5-CpOH proton transfer (by 9.0 kcal/mol in the gas phase). According to experimental results the analogue of **4f** is stable at 140 °C in toluene; this is supported by theoretical calculations because this species is very stable (−37.7 kcal/mol with respect to initial reactants), representing a clear well in the potential energy surface. Under H_2 pressure the substrate was completely reduced. These last observations are more according to the σ-bond metathesis mechanism than the η^5-CpOH proton transfer from the **4f** substrate.

The overall stepwise $\eta^5 \rightarrow \eta^2$ mechanism for alkyne hydrogenation presents a barrier height of 33.6 kcal/mol (32.3 kcal/mol in solution) corresponding to the steps from **1f** to **ts2f**. The highest point in the potential energy surface corresponds to the hydride transfer (**ts2f**). If the second hydrogenation process is the σ-bond metathesis of the H_2 molecule, the energy profile of the catalytic cycle is smoother than through the η^5-CpOH proton-transfer pathway, because in the last case the relative barrier height for the proton transfer is significantly higher (7.0 vs 34.3 kcal/mol in the gas phase), although lower than the hydride-transfer transition state (**ts2f**).

The stepwise $\eta^5 \rightarrow \eta^2$ mechanism in alkene hydrogenation presents a barrier height for the overall process of 30.1 kcal/mol (29.6 kcal/mol in solution), corresponding to the processes from **7f** to **ts2g** (hydride-transfer step).

Table 3. Relative Energies (in kcal/mol) in the Gas Phase (E_{B3LYP}) and Solution (E_{THF}) for the Concerted Outer-Sphere Mechanisms of Alkyne and Alkene Hydrogenation

	structure	E_{B3LYP}	E_{THF}
reactants	**a2** + **HC≡CH**	0.0	0.0
	1f	−6.0	−2.9
concerted transfer	**ts1d**	13.3	15.6
	2d	−31.2	−29.2
products	**b** + **H_2C=CH_2**	−27.3	−28.9
reactants	**a2** + **H_2C=CH_2**	0.0	0.0
	7f	−4.9	−1.6
concerted transfer	**ts1e**	14.5	16.3
	2e	−19.8	−18.6
products	**b** + **H_3C−CH_3**	−15.4	−17.7

The other possibility suggested by Casey for alkene hydrogenation,[18] which is initiated with the loss of one CO molecule, was not considered due to the highly reported energy value for the CO dissociation process.[20,37]

Outer-Sphere Mechanism for Alkyne and Alkene Hydrogenation. An analogous concerted outer-sphere mechanism localized for carbonyls and imines was also evaluated for alkynes and alkenes. The relative energies in both the gas phase and solution for the different intermediates of the concerted outer-sphere mechanism for alkyne and alkene hydrogenation are summarized in Table 3. For the alkynes, the barrier is significantly high, 19.3 kcal/mol (18.5 kcal/mol in solution), compared to polar double bonds, although it is the most feasible mechanism among those evaluated for the nonpolar multiple bonds. The related transition state (**ts1d**) is characterized by Ru−H and O−H distances of 1.672 and 1.041 Å, respectively, whereas the incoming C−H bonds are characterized by distances of 1.527 and 1.637 Å, respectively. These distances show a small variation of the catalyst structure when reaching the transition state; therefore, the proton of the CpOH group is less transferred than in polar double-bond hydrogenation. In Figure 9 are shown the transition states for the concerted outer-sphere mechanisms of alkyne (**ts1d**) and alkene (**ts1e**) hydrogenation.

Concerning the outer-sphere mechanism in alkene hydrogenation, the energy barrier is very similar to that of the alkynes, 19.4 kcal/mol (17.9 kcal/mol in solution). The related transition state (**ts1e**) is characterized by O−H and Ru−H distances of 1.101 and 1.727 Å, respectively, whereas the respective C−H distances are 1.514 and 1.401 Å.

These results show that the concerted outer-sphere mechanisms for alkynes and alkenes are around 10 kcal/mol higher in energy than the analogous ones in carbonyl and imine hydrogenations. This explains why polar double bonds react faster than multiple carbon−carbon bonds.

From all the results obtained for alkyne and alkene hydrogenation it can be concluded that the concerted outer-sphere mechanism is the most favorable pathway in both cases. Their relative barrier heights in the gas phase are 19.3 kcal/mol (18.5 kcal/mol in solution) and 19.4 kcal/mol (17.9 kcal/mol in solution), respectively. In alkyne hydrogenation, the formation

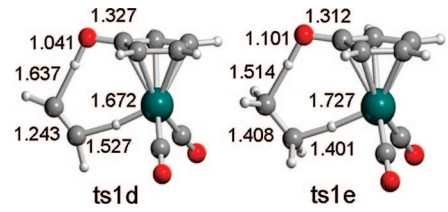

Figure 9. Transition states for the concerted outer-sphere mechanisms for HC≡CH (**ts1d**) and H_2C=CH_2 (**ts1e**) hydrogenations. Distances are in Å.

of **d** species proposed by Shvo can compete with the hydrogenation reaction, because of its relatively affordable energy barrier height of 22.8 kcal/mol (27.4 kcal/mol in solution) and the exothermicity of the process (−39.9 kcal/mol in the gas phase; −38.4 kcal/mol in solution).

Conclusions

The reaction mechanisms for the hydrogen tranfer to C═N, C═C, and C≡C bonds catalyzed by the Shvo catalyst have been extensively analyzed, complementing our previous theoretical study on the C═O hydrogenation.[20] Both suggested mechanisms, inner- and outer-sphere mechanisms, along with some variations have been computationally evaluated.

Our results show that the most favorable pathway for imine hydrogenation is the outer-sphere mechanism, which presents the lowest energy barrier of all the studied mechanisms. Similar results were previously found for the hydrogenation of carbonyls.[20] This conclusion is consistent independently of the selected system used for the calculations. Thus, calculations on a model catalyst and model imine in the gas phase show that the outer-sphere mechanism is the most feasible one with a barrier of 11.0 kcal/mol. The use of the complete catalyst (including the phenyl rings on the CpOH ligand) lead to the same conclusion (energy barrier of 9.3 kcal/mol). The effect of solvent, by means of both single-point calculations and geometry optimizations, is proven to be unremarkable (energy barriers of 7.1 and 6.8 kcal/mol, respectively). It should be noted, however, that the inclusion of solvent effects and phenyl rings (the latter to a minor extent) causes asynchronicity in the transition state, with the proton more transferred than the hydride. The same conclusions are found for the case of an imine with electron-donating groups: the energy profile obtained by geometry optimizations including solvent effects on the complete catalyst gives an energy barrier of 4.0 kcal/mol with an asynchronic transition state for the concerted outer-sphere mechanism. Thus, the energy barrier for the outer-sphere mechanism is lower than for the inner-sphere mechanisms in all the studied cases.

For multiple carbon−carbon bonds the most favorable hydrogenation mechanisms using the Shvo catalyst are also the outer-sphere mechanisms. Hydrogenation of nonpolar multiple bonds presents energy barriers approximately 10 kcal/mol higher than polar double bonds, having values of 18.5 and 17.9 kcal/mol for ethyne and ethene hydrogenations in solution, respectively. The difference between the outer-sphere mechanism and the most favorable inner-sphere mechanism is reduced in alkyne and alkene hydrogenation compared to those for polar double-bond hydrogenation. For the case of alkyne hydrogenation, the route proposed by Shvo that leads to catalyst deactivation has been calculated. On the basis of the relative energy barriers and the exothermicity of the process, this secondary reaction can compete with the hydrogenation reaction.

The energy differences for the outer-sphere mechanisms between polar double bonds and multiple carbon−carbon bonds agree with the observed chemoselectivity for polar double-bond hydrogenation over multiple carbon−carbon bond hydrogenation. According to these results, hydrogenation reactions of polar and nonpolar multiple bonds take place through an outer-sphere mechanism where the former substrates hydrogenate more easily, in agreement with experiment.

Acknowledgment. We are grateful to the Spanish MEC (Projects CTQ2005-09000-C02-01 and Consolider Ingenio 2010 CSD2007-00006, "Ramón y Cajal" contract to G.U. and FPU fellowship to A.C.-V.), as well as to the Generalitat de Catalunya (2005/SGR/00896).

Supporting Information Available: Complete ref 28, absolute energies, and Cartesian coordinates. This material is available free of charge via the Internet at http://pubs.acs.org.

OM700975K

(37) At high temperatures, this mechanism cannot be discarded.